Salahaddin University- Erbil

College of Science

Department of Earth Sciences & Petroleum

4ᵗʰ stage Research Project

2D Electrical Resistivity Tomography for the Investigation of the Subsurface Structures at the Shaqlawa Proposed Dam Site at Erbil Governorate, NE Iraq

Research Project
Submitted to the department of (Earth Sciences and Petroleum) in partial fulfillment of the requirements for the degree of BSc. in Earth Sciences and Petroleum.

Prepared by:

Evan Sherzad Younis   **Zainab Khalis Othman**

Supervised by:

Sirwa Qader Smail

Erbil-Kurdistan

April-2024

Abstract

Two-dimensional Electrical Resistivity Tomography (ERT) method was used to investigate a Dam site in Shaqlawa-Erbil Governorate, NE Iraq, to delineate the nature of the subsurface structures to assess its suitability for the construction of dam. The main objectives are to investigate the depth to the bedrock, possible geologic structures, such as possible presence of faults, fractures, voids and clay in the dam axis and abutments. The selected method has the possibility to give an image of the subsurface and map lateral and vertical variations in the subsurface geology of the site. For this purpose, the (SYSCAL Switch and SYSCAL Pro Switch units) equipment was used with Wenner array (48 electrodes). Three 2D electrical resistivity tomography profiles were conducted, the space between electrodes is 5m and the length of the profiles are 235 m. The depth of the investigation is assumed to be 40 m. The acquired data were inverted to tomogram sections using tomographic inversion by using TomoLAB commercial software. The Tomography sections show that the subsurface is classified into three distinct geo-electric layers, with different resistivity values; starting with high to moderate resistivity value represents unconsolidated coarse materials such as boulder and gravel, while in some location fine soft materials such as silty clay has been appeared that is underlain by a second layer of high resistivity has been detected within upper Fars (Injana) Formation; it is mainly composed of sandstone saturated and/or compacted. The third layer has low resistivity which represents the fine materials deposition of the Upper Fars Formation. The results showed that the site is suitable for the construction of the proposed dam.

List of contents

List of figures

List of tables

Chapter one

Introduction

1.1   preface

In the resistivity method, artificially generated electric currents are introduced into the ground and the resulting potential differences are measured at the surface. Deviations from the pattern of potential differences expected from homogeneous ground provide information on the form and electrical properties of subsurface inhomogeneities (Keary et. al, 2002).

Electrical resistivity methods were developed in the early 1900s but have become very much more widely used since the 1970s, due primarily to the availability of computers to process and analyze the data. These techniques are used extensively in the search for suitable groundwater sources and also to monitor types of groundwater pollution; in engineering surveys to locate subsurface cavities, faults and fissures, permafrost, mine shafts, and so on; and in archaeology for mapping out the areal extent of remnants of buried foundations of ancient buildings, amongst many other applications. Electrical resistivity methods are also used extensively in downhole logging (Reynolds, 2011).

The resistivity of rocks usually depends upon the amount of groundwater present and on the amount of salts dissolved in it, but it is also decreased by the presence of many ore minerals and by high temperatures (Musset and Aftab Khan, 2000).

1.2 Location of the study area

The study area is located in Erbil governorate which far away about 58 km to the Erbil city with northeast direction and about 3km northeast of Lassa village at shaqlawa area and with coordinate UTM time zone X=446165 and Y=4026368 (Fig.1).
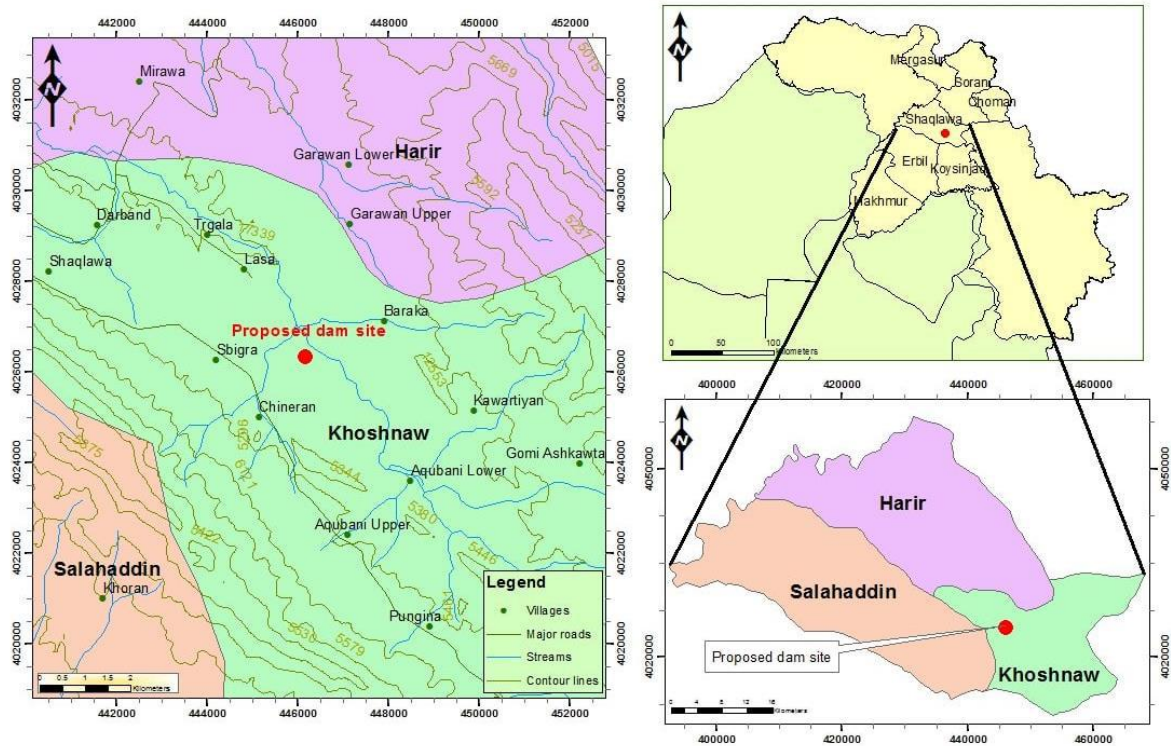
Figure 1.1: Location map of the study area.

1.3 Geology and structural setting

1.3.1 Tectonic and structure

Tectonically, the studied area located in the High Folded Zone of the Unstable Shelf tectonic zone of the Arabian Platform (Buday and Jassim 1987, Buday and Jassim 1984) (Fig. 2). It is characterized by intense folding and orogenic uplift, with closely packed narrow anticlines and synclines, this zone was the site of deposition of Paleocene molasses sediments (Buday 1980). Safeen anticline is one of the major anticlines in the high folded zone, which is an asymmetrical anticline, on-plane, and axial surface is directed (NW), gently double plunging fold with south-westward, trending NW-SE parallel to the Zagros Mountain Belt. Safeen Anticline is in the High Folded Zone, located about 45 km north east of Erbil city.
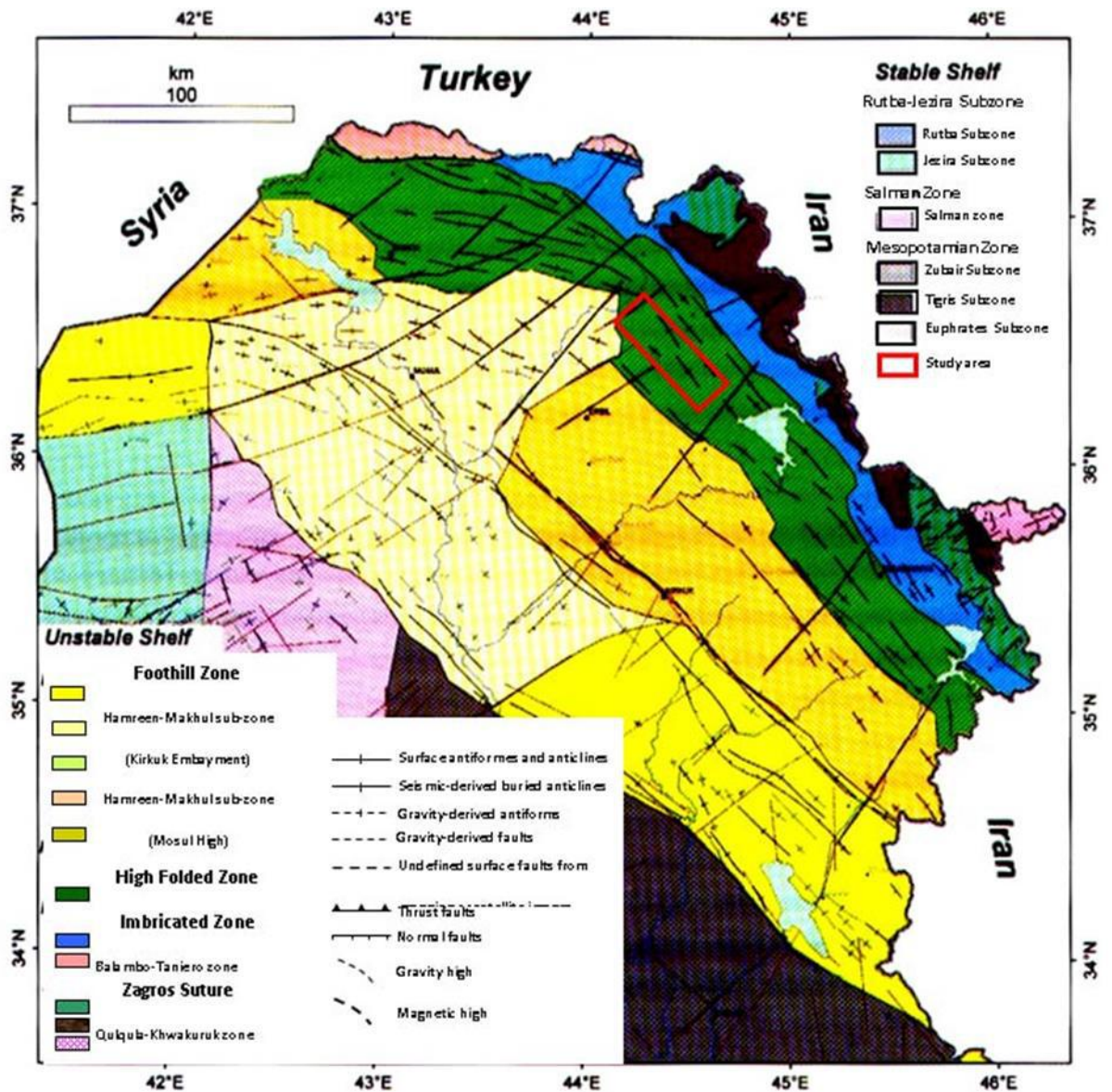
Figure 1.2: Tectonic zones and structural elements of unstable shelf units (Jassim and Goff, 2006).

1.3.2 Geology

Several different rock formations are exposed within the Shaqlawa dam area. The exposed Formations range in age from Cretaceous to Tertiary. The most important are Quaternary (Recent) deposites and Upper Fars (Injana) U-Miocene sediments (Fig. 1.3). The proposed dam site is exactly located on those formations, while other Formations are of lesser interests because most of them are exposing as small patches at the margins of the catchment area.

QUATERNARY

Q^f	Flood plain deposits	Siltstone and sandstone with lenses of claystone and conglomerate
Q^r	Residual soil and polygenetic deposits	Silty and clayey soil, locally gypsiferous or pebbly
Q^s	Slope deposits	Rock fragments, with fine clastics
Q^{af}	Alluvial fan deposits	Rock fragments, locally gravelly, covered by thin mantle of soil
	River terraces	Conglomerate with lenses of sandstone and siltstone

TERTIARY

Pli^b	Bai Hassan (Upper Bakhtiari) Formation	Conglomerate, sandstone and claystone
Mio_3-Pli^m	Mukdadiyah (Lower Bakhtiari) Formation	Pebbly sandstone, siltstone and claystone
Mio_3^i	Injana (Upper Fars) Formation	Sandstone, siltstone and claystone
Mio_2^f	Fatha (Lower Fars) Formation	Gypsum, marl, limestone, red claystone and siltstone
Eoc_{2-3}^p	Pilaspi Formation	Mainly well bedded limestones
Eoc_{2-3}^a	Avanah Formation	Mainly well bedded limestones
Eoc_{1-2}^g	Gercus Formation	Red sandstone, siltstone and claystone
$Pal_2-Eoc_1^k$	Khurmala Formation	Mainly well bedded limestones
Pal_{1-2}^{ko}	Kolosh Formation	Black claystone, siltstone and sandstone

CRETACEOUS

K_2^t	Tanjero Formation	Khaki sandstone and claystone, with conglomerate
K_2^s	Shiranish Formation	Well bedded limestones and blue marl
K_2^{be}	Aqra–Bekhme Formation (locally with Kometan Formation)	Mainly well bedded to massive limestones (Marly limestone)
K_1^{qa}	Qamchuqa Formation	Mainly massive limestones and dolomites
K_1^{ba}	Balambo, Garagu and Sarmord Formations	Marly limestone, marl, bedded limestone and dolomite

JURASSIC

$J2$	Chia Gara, Barsarin, Naokelekan and Sargelu Formations	Mainly bedded to massive dolomites, limestone and marl
$J1$	Sehkaniyan and Sarki Formations	Mainly limestone, dolomite, thin bedded limestone and shale

GEOLOGICAL SYMBOLS

- Geological contact
- Axis of anticline
- Axis of over turned anticline
- Axis of syncline
- Thrust fault
- Fault with down thrown side
- Fault (other types)

TOPOGRAPHICAL SYMBOLS

- Paved road
- Contour line
- Triangulation point with number and height . Spot height
- Town . Village
- River
- Valley
- Bridge   Quarry

Figure 1.3: Geological map of the studied area (Sissakian et. al, 1997).

- **Recent deposits (Quaternary)**
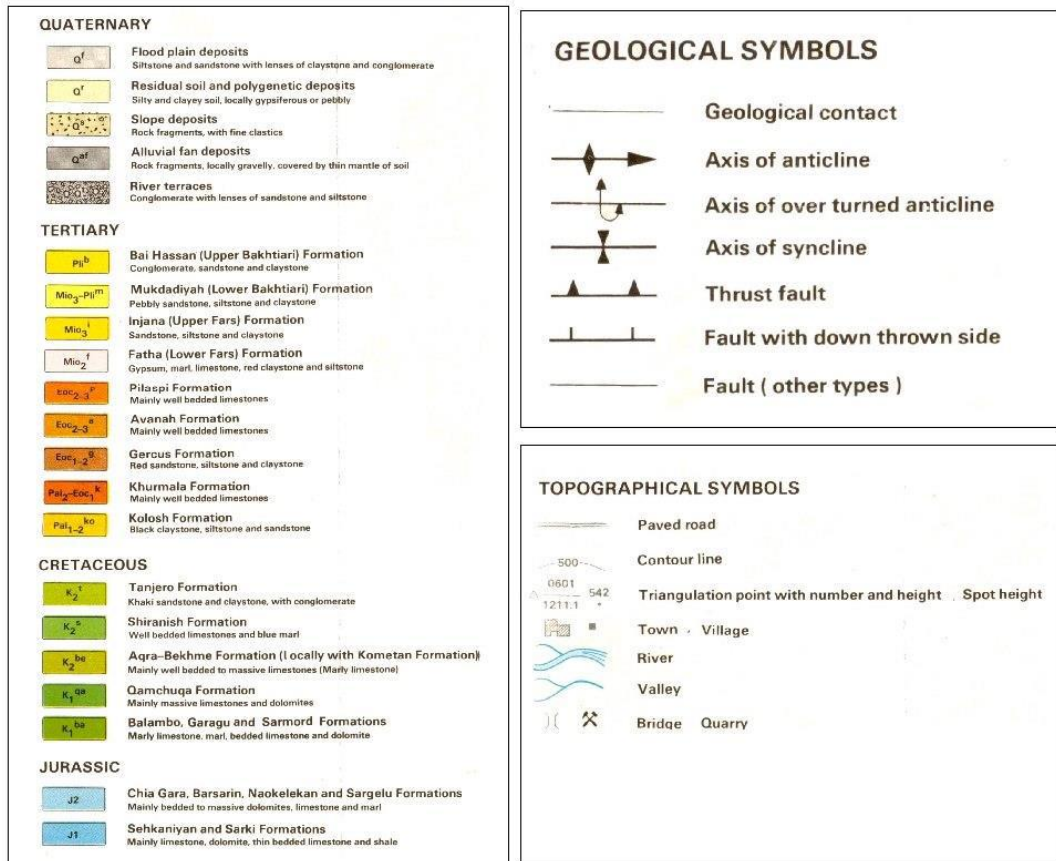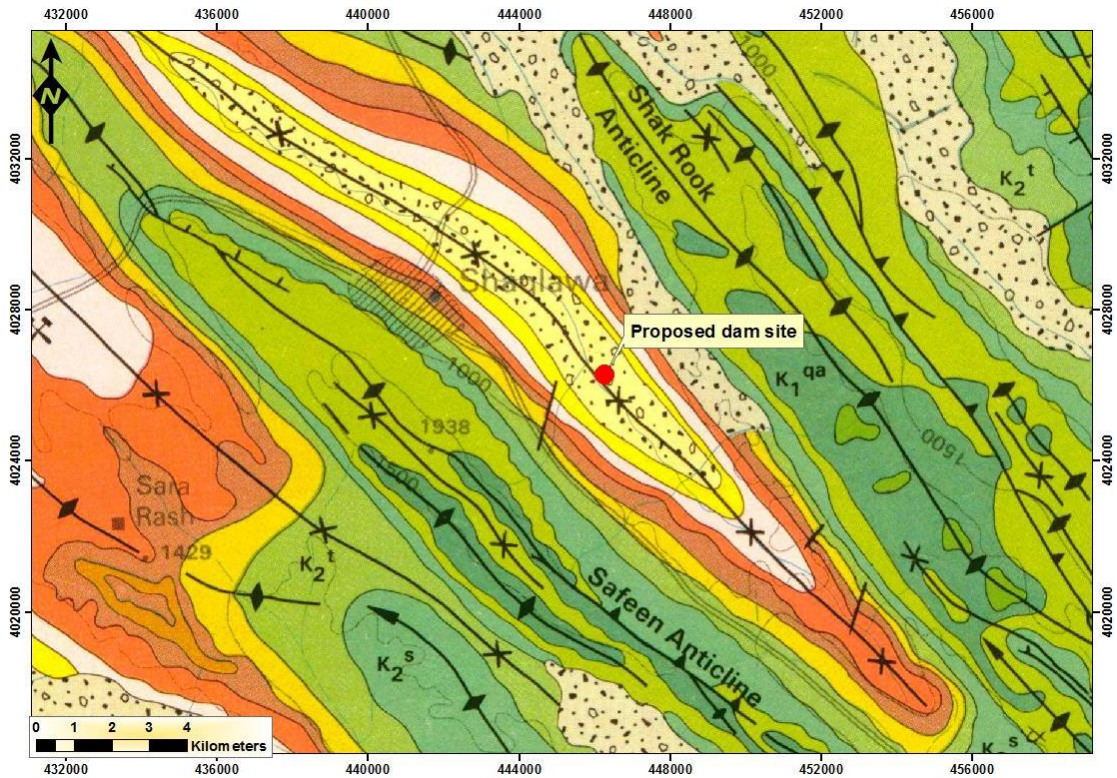
These deposits exposed in all parts of the proposed dam area. It is mainly consisting of clayey and silty types, with dominant reddish brown colour, which are derived from older formations, Locally, pebbles and some rock fragments occur within the soil generally limestone pebbles, up to 25 cm in diameter derived from the Pila Spi Formation, occur within these deposits (Jassim and Goff, 2006).

- **Upper Fars formation (Injana) U-Miocene**

The upper Fars formation was originally described in the Fars province of Iran but without a type locality in Iraq. The age of the formation is Late Miocene. This formation exposed in the core of synclines within the study region. This formation mainly consists of marl, siltstone, mudstone and sandstone whose size vary from medium to coarse and claystone whereas limestone and shale exist in lower part of the formation (Buday, 1980). The studied area is covered by this formation shown in (Fig. 1.3).

- **Lower Fars formation (Fat'ha) M-Miocene**

This formation mainly consists of alternation of evaporates (gypsum and anhydrite), marl (calcareous shale) sandstone and red claystone with possible limestone. The sandstone and red claystone beds are exposed only in the periphery of the basin while evaporates, carbonate and marl occur mainly in the center of the basin. The upper contact is gradational with Injana (previous Upper Fars) Formation and most probably (somewhat) diachronous (Bellen, et. al, 1959).

1.4 The aim of this study

The goal of this study is to conduct a geophysical survey (Electrical Resistivity Tomography) of the study area to see if there are any structures, faults, cavities or fractures in the subsurface because if there is any structure, it will affect the dam, if the water leaks, the place will collapse and the dam will failure in the future, the importance of geophysical survey is to spend less money and time without interrupting the environment.

Chapter Two

Theoretical Background of 2D Resistivity Imaging

2.1 Principle and theory of Electrical Resistivity Method

Direct current (dc) resistivity methods use artificial sources of current to produce an electrical potential field in the ground. In almost all resistivity methods, a current is introduced into the ground through point electrodes (C1, C2) and the potential field is measured using two other electrodes (the potential electrodes P1 and P2). The source current can be direct current or low-frequency (0.1 - 30 Hz) alternating current. The aim of generating and measuring the electrical potential field is to determine the spatial resistivity distribution (or its reciprocal - conductivity) in the ground. As the potential between P1 and P2, the current introduced through C1 and C2, and the electrode configuration are known, the resistivity of the ground can be determined; this is referred to as the "apparent resistivity" (Knodel et. al, 2007).

For most materials, including most rocks, the current through a piece of the material increases in proportion to the p.d (potential difference). (Fig. 2.1): For example, doubling the p.d. doubles the current. (Fig. 2.1a) shows how these could be measured: The voltmeter measures the p.d. across the ends of the piece, while the ammeter measures the current flowing through it (the voltmeter is designed so that a negligible fraction of the current flows through it, and the parts are connected by wires with small resistance, so the effects of the connecting circuitry are minimized). This simple proportion of current to p.d. is called Ohm's Law. The amount of current flowing when the p.d. is 1 volt is called the resistance of the piece; it also equals the slope of (Figure 2.1b). Resistance is measured in ohms (given the symbol Ω). As an equation, Ohm's Law is (Musset and Aftab Khan, 2000):

$$\frac{potential\ or\ voltage\ difference\ (volts)}{current\ (amps)} = \frac{V}{I} = \text{resistance R (ohms)} \qquad \text{Ohm's}$$
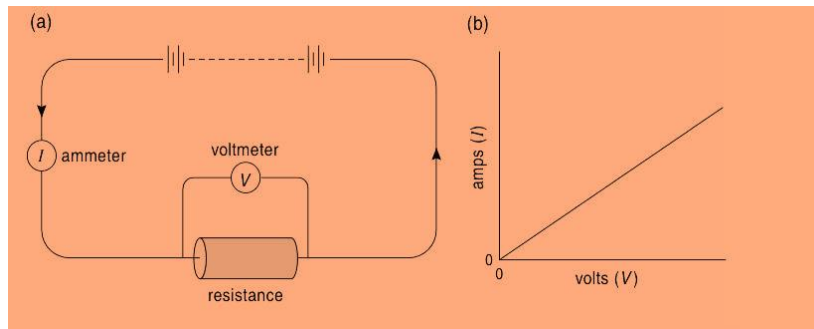
Law   Eq. 2.1

Figure 2.1: Measuring resistance (Musset and Aftab Khan, 2000).

The value of resistance depends upon both the material and its shape; a wire of copper has less resistance than one of lead with the same dimensions, while a long thin wire has greater resistance than a short, fat one of the same materials: doubling the length doubles the resistance, but doubling the area of cross-section halves it, just as doubling the cross-sectional area of a pipe would double the rate of water flow through it (Fig. 2.2). For a uniform bar (Fig. 2.3) these effects can be summarized as follows (Musset and Aftab Khan, 2000):

$$\text{Resistance (R)} = \text{resistivity } (\rho) \times \frac{length}{area\ of\ cross-section} \qquad \text{Eq. 2.1a}$$

$$\text{Resistivity } (\rho) = \text{resistance} \times \frac{area\ of\ cross-section}{length} \qquad \text{Eq. 2.1b}$$
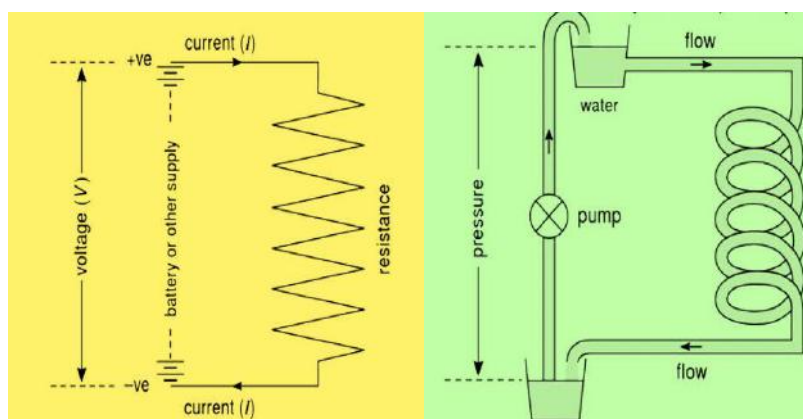

Figure 2.2: Analogy between electricity and water (Musset and Aftab Khan, 2000).

7
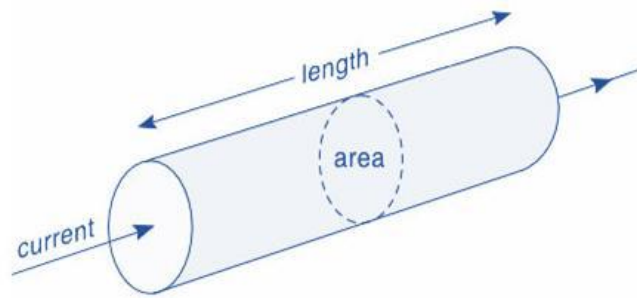
Figure 2.3: Resistance of a wire depends partly on its dimensions (Musset and Aftab Khan, 2000).

2.2 Applications of electrical Resistivity method

The application of the resistivity survey to environmental and geotechnical problems (From Knodel et. al, 2007):

1. Investigation of lithological underground structures.

2. Estimation of depth, thickness and properties of aquifers and aquicludes.

3. Determination of the thickness of the weathered zone covering unweathered rock.

4. Detection of fractures and faults in crystalline rock.

5. Mapping of preferential pathways of groundwater flow.

6. Localization and delineation of the horizontal extent of dumped materials.

7. Estimation of depth and thickness of landfills.

8. Detection of inhomogeneities within a waste dump.

9. Mapping contamination plumes.

10. Monitoring of temporal changes in subsurface electrical properties.

11. Detection of underground cavities.

12. Classification of cohesive and non-cohesive material in dikes, levees, and dams.

2.3 Apparent resistivity and current flow

In the resistivity survey, the ratio of current to p.d., $\Delta V/I$, is measured with increasing electrode separations. This ratio changes for two reasons, because of changes of resistivity with depth but also simply because the electrodes are being moved apart (Musett and Aftab khan, 2000).

- **Current flow in a homogeneous area**

For a single current electrode implanted at the surface of a homogeneous medium of resistivity ρ, current flows away radially (Fig. 2.4). The voltage drop between any two points on the surface car be described by the potential gradient ($-\delta V/\delta x$), which is negative because the potential decreases in the direction of current flow. Lines of equal voltage ('equipotentials') intersect the lines of equal current at right-angles. The current density (J) is the current (I) divided by the area over which the current is distributed (a hemisphere; $2\pi r2$), and so the current density decreases with increasing distance from the current source. It is possible to calculate the voltage at a distance (r) from a single current point source (Reynolds, 2011). The potential difference (δV) across a hemispherical shell of incremental thickness δr is given by:

$$\frac{\delta V}{\delta r} = -\rho \cdot J = -\rho \frac{I}{2\pi^2 r}.$$

Thus the voltage Vr at a point r from the current point source is:

$$V_r = \int \delta V = -\int \rho \cdot \frac{I\delta r}{2\pi r^2} = \frac{\rho I}{2\pi} \cdot \frac{1}{r}.$$
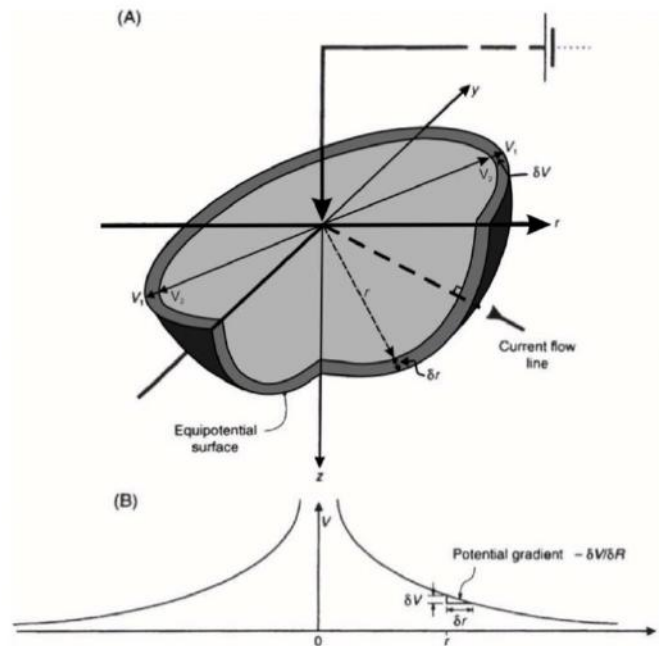
Figure 2.4: (A) Three-dimensional representation of a hemispherical equipotential shell around a point electrode on a semi-infinite, homogeneous medium. (B) Potential decay away from the point electrode (Reynolds, 2011).

If, however, a current sink is added, a new potential distribution occurs (Fig. 2.6) and a modified expression is obtained to describe the voltage at any point (Reynolds, 2011).

Figure 2.5: Current and equipotential lines produced by a current source and sink (Reynolds, 2011).

- **Function of apparent resistivity:**

For a current source and sink, the potential Vp at any point P in the ground is equal to the sum of the voltages from the two electrodes, such that: Vp = VA + VB where VA and VB are the potential contributions from the two electrodes, A(+I) and B(-I).

The potentials at electrode M and N are (Reynolds, 2011):

$$Vm = \frac{\rho I}{2\pi}\left(\frac{1}{AM} - \frac{1}{MB}\right), \quad Vn = \frac{\rho I}{2\pi}\left(\frac{1}{AN} - \frac{1}{NB}\right)$$
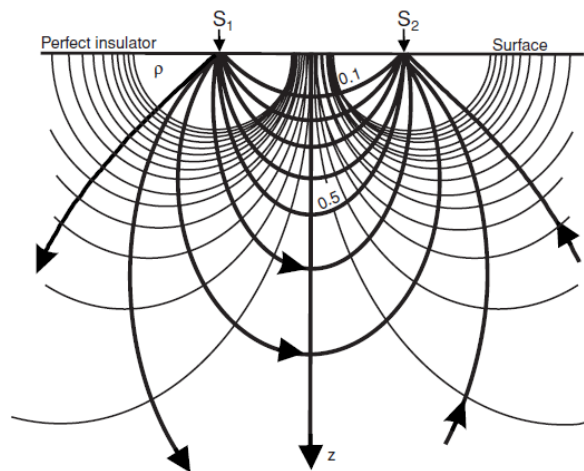
However, it is far easier to measure the potential difference, δVMNwhich can be rewritten as: $\rho VMN = VM - VN \equiv \frac{\rho I}{2\pi}\langle(\frac{1}{AM} - \frac{1}{MB}) - (\frac{1}{AN} - \frac{1}{NB})\rangle$

Rearranging this so that resistivity ρ is the subject:

$$\rho = \frac{2\pi\rho Vmn}{I}\langle(\frac{1}{AM} - \frac{1}{MB}) - (\frac{1}{AN} - \frac{1}{NB})\rangle^{-1}$$

The geometric factor (K; units m) see in (Fig 2.6). In reality, the subsurface ground does not conform to a homogeneous medium and thus the resistivity obtained is no longer the 'true' resistivity but the apparent resistivity (Pa), which can even be negative. It is very important to remember that the apparent resistivity is not a physical property of the subsurface media, unlike the true resistivity (Reynolds, 2011).
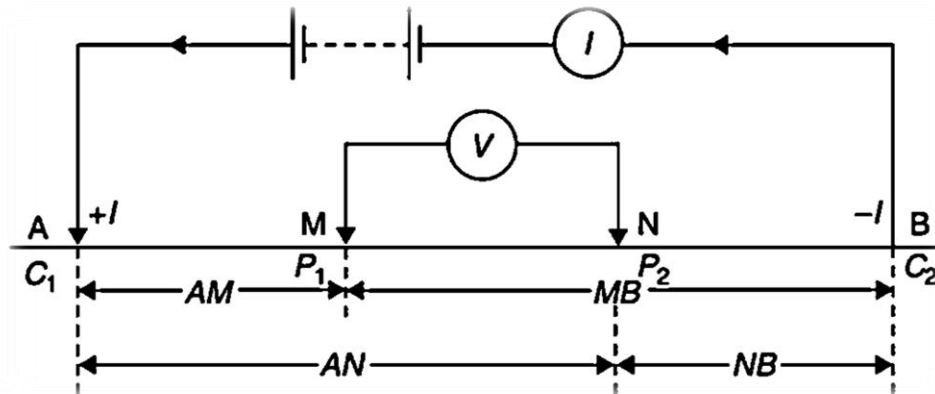

Figure 2.6: Generalized form of electrode configuration in resistivity surveys (Reynolds, 2011).

The geometric factor (K) is defined by the expression:

$$K = 2\pi \left(\frac{1}{AM} - \frac{1}{MB} - \frac{1}{AN} + \frac{1}{NB} \right)$$

Where the ground is not uniform, the resistivity so calculated is called the apparent resistivity ($\rho\alpha$):

$\rho\alpha = R\,k, where\ R = \delta V / I$

- **Refraction of current paths**

Within a uniform layer the current paths are smooth curves (as shown in Fig. 2.5), but they bend, or refract, as they cross an interface separating different resistivities. They refract towards the normal when crossing into rock with higher resistivity (Fig. 2.7a), and conversely in rock with lower resistivity (Fig. 2.7b) (Musett and Aftab khan, 2000).
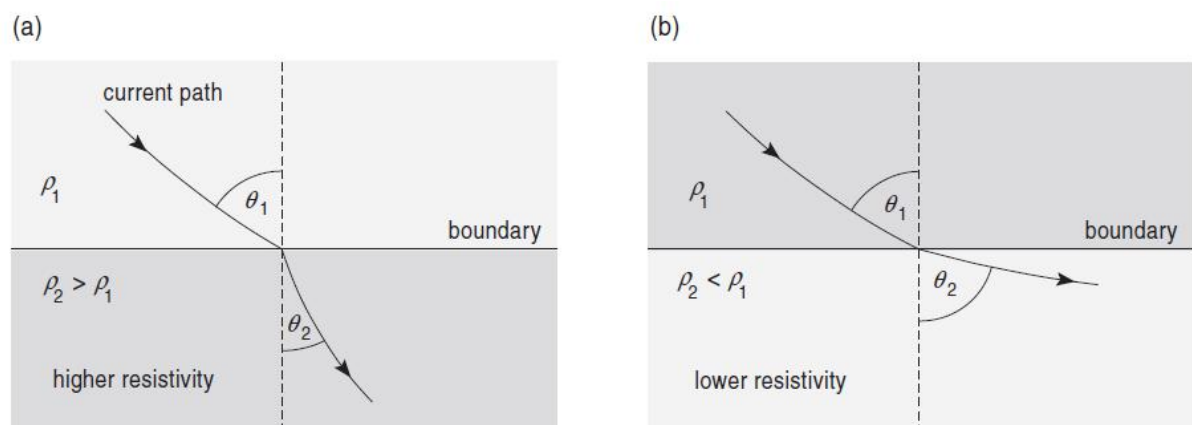
Figure 2.7: (A) When they refract towards the normal when crossing into rock with higher resistivity. (B) When conversely in rock with lower resistivity (Musett and Aftab khan, 2000).

2.4 Electrode arrays

The value of the apparent resistivity depends upon the geometry of the electrode array used, as defined by the geometric factor K. There are at least 102 different surface array types now recognized, most of which are rarely used; There are three main types of electrode configuration in common use, two of which are named after their originators – Frank Wenner and Conrad Schlumberger (Reynolds, 2011).
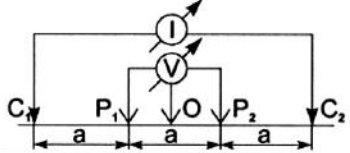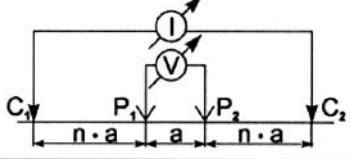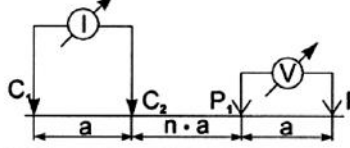
- **Choosing a resistivity array**

These different types and styles of electrode configuration have particular advantages, disadvantages and sensitivities. Factors affecting the choice of array type include the amount of space available to lay out an array, and the labor intensity of each method. Other important considerations are the sensitivity to lateral inhomogeneities and to dipping interfaces. It is important to recognize the advantages and disadvantages of each array; the choice of array is often a function of the user's previous familiarity with the array type, availability of cabling and data acquisition software, and of data processing and inversion software, as well as site-specific factors (Reynolds, 2011).

1. Wenner array

The method is extremely simple in concept. (Table 2.1) shows a single contribution section for a standard Wenner array. The four electrodes A, M, N, and B are equally spaced along a straight line. The distance between adjacent electrodes is called "a" spacing. This array is sensitive to horizontal variations (Reynolds, 2011).

Table 2.1: Some electrode arrays for dc resistivity measurements (Knodel, et. al., 2007)

Electrode array	Electrode configuration	Configuration factor
Wenner		$K = 2\pi\, a$
Schlumberger		$K = \pi\; n\,(n+1)\,a$ $n > 3$
dipole-dipole		$K = \pi\; n\,(n+1)\,(n+2)\,a$

2. Schlumberger array

The Schlumberger array differs from the Wenner array in having the P electrodes much closer together (Table 2.1), though still placed symmetrically about the center of the array. Readings are taken with only the current, C, electrodes being moved progressively and symmetrically apart. Moving only the C electrodes has two advantages: There are fewer electrodes to move, and with the P electrodes fixed the readings are less affected by any lateral variations that may exist. However, when expansion causes the value of ΔV to become so small that it cannot be measured precisely, the *P* electrodes are moved much further apart, while keeping the *C* electrodes fixed; then further readings are taken by expanding the *C* electrodes using the new *P* electrode positions. This array is less sensitive to lateral variations and faster to use as only the current electrodes are moved (Musset and Aftab Khan, 2000).

3. Dipole-dipole array

Dipole–dipole arrays have been used extensively by Russian geophysicists since 1950, and especially in Canada, particularly for 'induced polarization' surveys in mineral exploration, and in the USA in groundwater surveys. The distance between the current electrode A and B (current dipole) and the distance between the potential electrodes M and N (measuring dipole) are significantly smaller than the distance r, between the centers of the two dipoles (Table 2.1). This array type has a better horizontal resolution, but shallower investigation depth than the Wenner array (Reynolds, 2011).

2.5 Electrical resistivity survey techniques

Resistivity measurements may be made at the Earth's surface, between boreholes or between a single borehole and the surface. With special cables, measurements

can be made underwater in lakes, rivers and coastal areas. The following basic modes of operation can be used (knodel, et. al., 2007):

- profiling (mapping),
- vertical electrical sounding (VES),
- combined sounding and profiling (two-dimensional resistivity imaging)

- **Profiling (mapping)**

Profiling methods use fixed electrode spacing to detect lateral resistivity changes along a profile down to a more or less constant investigation depth, which is governed by the electrode spacing. The results are normally interpreted qualitatively. Contour maps or profile plots of the measured apparent resistivities allow delineation of lateral boundaries of geogenic structures and anthropogenic features (e.g., waste dumps and contamination plumes), as well as hydrogeological conditions.

- **Sounding mode (VES)**

Sounding methods is to determine the vertical distribution of the resistivity in the ground. Several soundings at regular spacing along profiles or randomly in the area under investigation will also provide information about the lateral extent of structures. Soundings may be made for investigation depths up to several hundred meters. The measured data may be interpreted both qualitatively and quantitatively. The latter will provide resistivity models whose layer boundaries are boundaries of geoelectrical layers but not necessarily of lithological layers. For a better correlation to the geology, geoelectrical data should be correlated with borehole logs or the results of other geophysical methods, such as reflection and refraction seismic sections.

- **Profile sounding (Two-dimensional resistivity imaging)**

Sounding and profiling can be combined in a single process (2-D resistivity imaging) to investigate complicated geological structures with strong lateral

resistivity changes. This combination provides detailed information both laterally and vertically along the profile and is the most frequently applied technique in environmental studies. 2-D inversion yields a two-dimensional distribution of resistivities in the ground.

2.6 Electrical resistivity tomography

We have seen that the greatest limitation of the resistivity sounding method is that it does not take into account horizontal changes in the subsurface resistivity. A more accurate model of the subsurface is a two-dimensional (2-D) model where the resistivity changes in the vertical direction, as well as in the horizontal direction along the survey line. In this case, it is assumed that resistivity does not change in the direction that is perpendicular to the survey line. In many situations, particularly for surveys over elongated geological bodies, this is a reasonable assumption. In theory, a 3-D resistivity survey and interpretation model should be even more accurate. However, at the present time, 2-D surveys are the most practical economic compromise between obtaining very accurate results and keeping the survey costs down (Dahlin 1996). Typical 1-D resistivity sounding surveys usually involve about 10 to 20 readings, while 2-D imaging surveys involve about 100 to 1000 measurements. In comparison, a 3-D survey might involve several thousand measurements. The cost of a typical 2-D survey could be several times the cost of a 1-D sounding survey, and is probably comparable with a seismic refraction survey. In many geological situations, 2-D electrical imaging surveys can give useful results that are complementary to the information obtained by other geophysical methods. For example, seismic methods can map undulating interfaces well, but will have difficulty (without using advanced data processing techniques) in mapping discrete bodies such as boulders, cavities and pollution plumes. Ground radar surveys can provide more detailed pictures but have very limited depth penetration in areas with conductive unconsolidated sediments, such as clayey soils. Two-dimensional electrical

surveys can be used in conjunction with seismic or GPR surveys as they provide complementary information about the subsurface (Loke, 2014).

2.7 Principle of multi-electrode resistivity imaging

For a few years, the evolution of electronic components and of computer processing have permitted to develop field resistivity equipment (SYSCAL Switch and SYSCAL Pro Switch units) which includes a large number of electrodes located along a line at the same time, and which carries out an automatic switching of these electrodes for acquiring profiling data. This technique, called Resistivity Imaging or Electrical Resistivity Tomography (ERT), finds applications in the environment, groundwater, civil engineering and archaeology fields. The images which are obtained (apparent resistivity pseudo sections) are processed by an inversion software which gives interpreted resistivity and depth values for the anomalies detected along the profile. The multi-electrode resistivity technique consists in using a multi-core cable with as many conductors (24, 48, 72, 96, ...) as electrodes plugged into the ground at a fixed spacing, every 5m for instance (Fig. 2.8). In the resistivity meter itself are located the relays which ensure the switching of those electrodes according to a sequence of readings predefined and stored in the internal memory of the equipment. The various combinations of transmitting (A,B) and receiving (M,N) pairs of electrodes construct the mixed sounding / profiling section Figure (2.9), with a maximum investigation depth which mainly depends on the total length of the cable. Various types of electrode combinations can be used, such as Dipole-Dipole, Wenner-Schlumberger, Pole-Pole arrays. Each type of combination has advantages and limitations in terms of lateral resolution and vertical penetration for instance, as summarized in Table (2.2) (https://www.iris-instruments.com/).
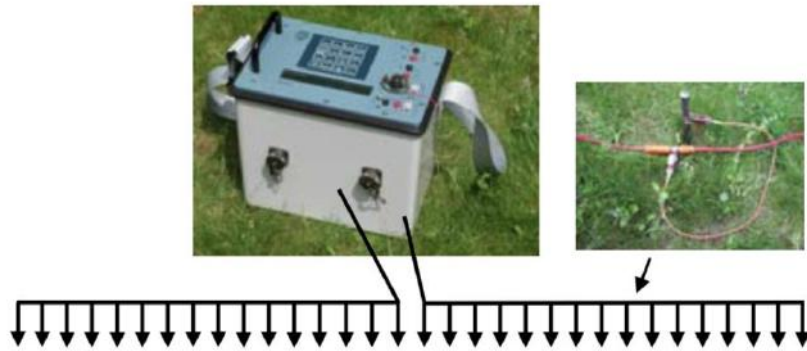
Figure 2.8: SYSCAL Switch multi-electrode equipment (https://www.iris-instruments.com/).
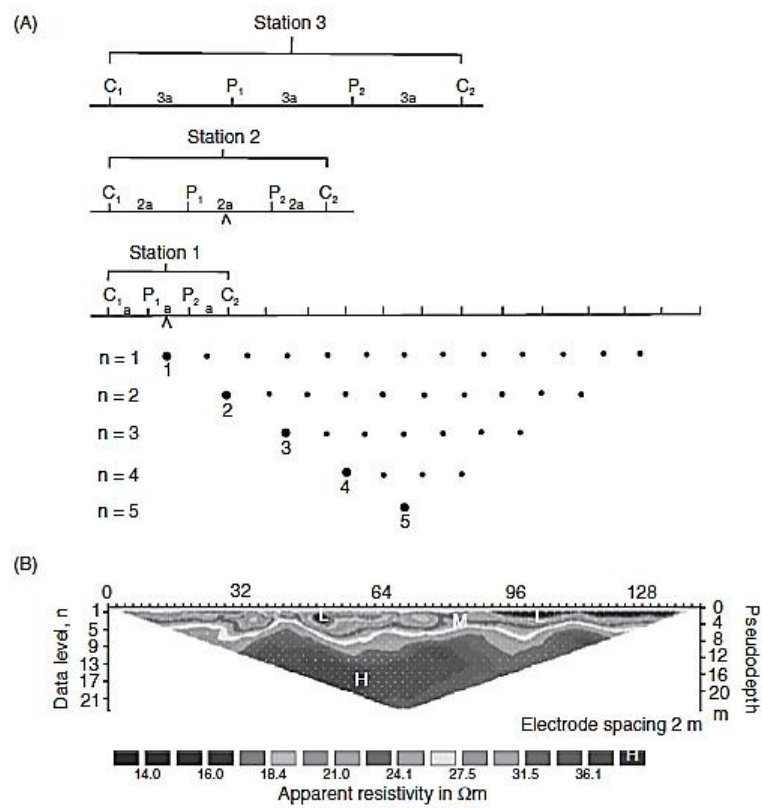

Figure 2.9: (A) Example of the measurement sequence for building up a resistivity pseudo-section. (B) Example of a measured apparent resistivity pseudo-section (Reynolds, 2011).

Table2.2: properties of electrode arrays (Bernard, et. al., http://www.iris-instruments.com/training.html).

Arrays		DIPOLE - DIPOLE	WENNER - SCHLUMB	POLE - POLE
Main criteria	Resolution Depth Field set-up	best weak regular	regular regular regular	weak best weak
Other criteria	Amplitude Natural noise Coupling noise	weak regular best	regular regular regular	best weak weak
CONFIGURATION		A B M N $\downarrow$ a $\downarrow$ na $\downarrow$ a $\downarrow$ $\longleftarrow$ L $\longrightarrow$	A M N B $\downarrow$ na $\downarrow$ a $\downarrow$ na $\downarrow$ $\longleftarrow$ L $\longrightarrow$	B A M N $\downarrow$ a $\downarrow$ $\leftrightarrow$ L
ESTIMATED INVESTIGATION DEPTH		about 0.2 x L	about 0.2 x L	about 0.9 x L

2.8 Depth of investigation of multi electrode resistivity imaging

In electrical methods, the depth of penetration is linked to the distance between electrodes. For a set of 48 electrodes spaced at 5m, two segments with 24 electrodes each are usually used, the resistivity meter being placed between both segments; the total length of the cables is 240m. In a first approximation, for Dipole Dipole, Schlumberger and Wenner arrays, the maximum depth of penetration is of the order of 20% of the total length of the cable, or 50m (Fig. 2.10). This depth is reached for the combination of the two extreme left and the two extreme right electrodes of the profile, and the measuring report plotting point corresponds to the bottom angle of the triangle of the pseudo section.

station
1

segment a   segment b

Max

AREA INVESTIGATED
with one set of readings of a multi-electrode
sequence. The equipment is placed in the middle
(station 1) of the multi-core cable composed of
two segments, a and b.

The maximum depth reached, referred to as
Max, depends on the electrode arrays used.
For Wenner and dipole dipole arrays, this Max
depth is estimated to 0.2 L, L being the total
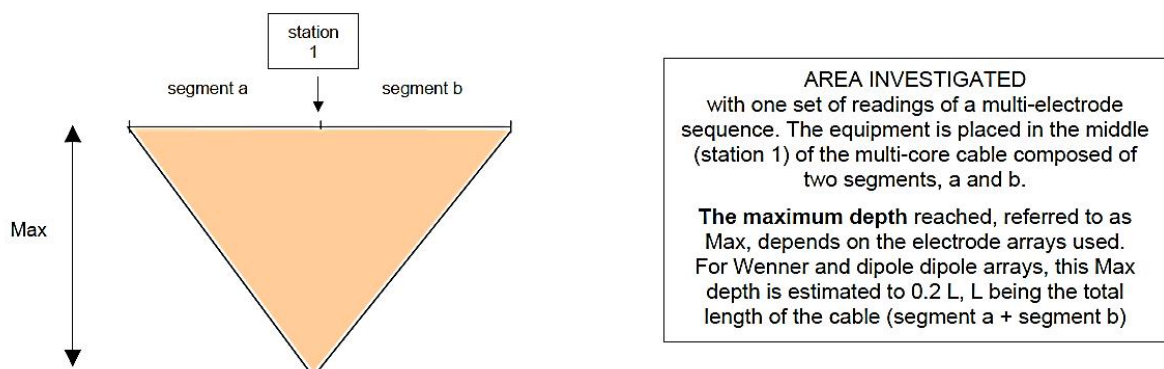length of the cable (segment a + segment b)

Figure 2.10: Depth of penetration in multi-electrode resistivity measurements (Bernard, 2003).

2.8 Resistivity of geological materials

Resistivity methods are useful only if the resistivity of the target differs significantly from the resistivity of the host material. For the successful planning of any geoelectrical survey and for the interpretation of the data, it is very important to know the resistivities of the materials in the study area. Resistivities of some selected materials, including typical domestic and industrial waste, are listed in (Table 2.3).

Table 2.3: Resistivities for geological and waste materials (Knodel, et. al., 2007)

Material	Resistivity (in Ωm)	
	minimum	maximum
gravel	50 (water saturated)	$>10^4$ (dry)
sand	50 (water saturated)	$>10^4$ (dry)
silt	20	50
loam	30	100
clay (wet)	5	30
clay (dry)		>1000
peat, humus, sludge	15	25
sandstone	<50 (wet, jointed)	$>10^5$ (compact)
limestone	100 (wet, jointed)	$>10^5$ (compact)
schist	50 (wet, jointed)	$>10^5$ (compact)
igneous and metamorphic rock	<100 (weathered, wet)	$>10^6$ (compact)
rock salt	30 (wet)	$>10^6$ (compact)
domestic and industrial waste	<1	>1000 (plastic)
natural water	10	300
sea water (35‰ NaCl)	0.25	
saline water (brine)	<0.15	

Igneous and metamorphic rocks typically have high resistivity values (Table 2.3). The resistivity of these rocks is greatly dependent on the degree of fracturing, and the percentage of the fractures filled with ground water. Thus a given rock type can have a large range of resistivity, from about 1000 to 10 million Ω.m, depending on whether it is wet or dry. This characteristic is useful in the detection of fracture zones and other weathering features, such as in engineering and groundwater surveys. Sedimentary rocks, which are usually more porous and have higher water content, normally have lower resistivity values compared to igneous

and metamorphic rocks. The resistivity values range from 10 to about 10000 Ω.m, with most values below 1000 Ω.m. The resistivity values are largely dependent on the porosity of the rocks, and the salinity of the contained water. Unconsolidated sediments generally have even lower resistivity values than sedimentary rocks, with values ranging from about 10 to less than 1000 Ω.m. The resistivity value is dependent on the porosity (assuming all the pores are saturated) as well as the clay content. Clayey soil normally has a lower resistivity value than sandy soil. However, note the overlap in the resistivity values of the different classes of rocks and soils. This is because the resistivity of a particular rock or soil sample depends on a number of factors such as the porosity, the degree of water saturation and the concentration of dissolved salts (Loke, 2014).

Pore fluids considerably reduce the resistivity of porous sediments (Table 2.3). The resistivity of a rock that is saturated with highly mineralized water can be significantly lower than given in (Table 2.3). Sandy sediments containing highly mineralized pore water can have the same resistivity as clay. In such cases it is difficult to distinguish between sand and clay layers on the basis of resistivity alone. Data from a combination of methods (e.g., induced polarization, seismic, ground penetrating radar) should be used to identify subsurface lithology and structures (knodel, et.al., 2007).

2.10 Noise:

Resistivity measurements in populated areas can be disturbed by various noise sources, such as grounded metal fences, underground metal pipes and cables, power lines, electric corrosion protection for pipelines or leakage currents generated by industrial facilities, streetcars and trains. Especially underground metal pipes can produce anomalies which influence the interpretation quite seriously. If it is unavoidable to measure in such an area, it is better for the profiles to be perpendicular to the pipes than parallel to them (Knodel, et. al., 2007).

Chapter three

Data acquisition and interpretation

3.1 The operating procedure in resistivity imaging techniques

One of the new developments in recent years is the use of 2-D electrical Tomography surveys to map areas with moderately complex geology (Griffiths and barker,1993). Such surveys are usually carried out using a large number of electrodes, in this survey 48 electrodes were used, connected to a multi-core cable. A laptop microcomputer together with an electronic switching unit is used to automatically select the relevant four electrodes for each measurement. Normally a constant spacing between adjacent electrodes is used. The multi-core cable is attached to an electronic switching unit which is connected to a laptop computer (Bernard, et. al., (https://www.iris-instruments.com/). The procedure for getting resistivity imaging includes the following four successive steps:

- Creating the sequence of measurements with a PC software; the sequence depends on the number of electrodes, their spacing. the type of array (Schlumberger-Wenner, Dipole-Dipole, Pole Dipole, Pole Pole...). the investigation depth to reach; loading of this sequence into the memory of the resistivitymeter.

- Taking the readings in the field, after the electrode resistance checking, and the introduction of the stack number which depends on the signal to noise ratio.

- During the measurements, the output voltage of the equipment is automatically adjusted to the level of the signal measured.

- Transferring the data from the memory of the equipment to a PC, filtering of noisy data in relation with their standard deviation or on the level of the signal, introduction of the topography (electrode elevation), visualization of the results by level of investigation depth.

Inverting the data with a PC 2D software, which, after a certain number of iterations, gives the values of the interpreted resistivities (through a color scale), and depths (https://www.iris-instruments.com/).

3.2 Data acquisition and instruments

One of the new developments in recent years is the use of 2-D electrical Tomography surveys to map areas with moderately complex geology (Griffiths and R.D. Barker,1993). Such surveys are usually carried out using a large number of electrodes, in these surveys 48 electrodes were used, connected to a multi-core cable. A laptop microcomputer together with an electronic switching unit is used to automatically select the relevant four electrodes for each measurement. Normally a constant spacing between adjacent electrodes is used. The ERT measurements were carried out along three profiles in May 2013 at Shaqlawa proposed dam site (Fig. 3.1 and 3.3), with standard Wenner-schlumberger array (48 electrodes); the space between electrodes is 5m and the length of each profile is 235 m, and the depth of the investigation is assumed to be 40 m. The equipment (SYSCAL Switch and SYSCAL Pro Switch units) was used which includes a large number of electrodes located along a line at the same time, and which carries out an automatic switching of these electrodes for acquiring profiling data (Fig. 3.2). The effect of the topography must be taken into account when carrying out an inversion of the data set. For that reason, during the survey at the field the elevations of the electrodes were measured along the profile where the elevation changed by twelve channels global positioning system (GPS) set- the "GARMIN GPS 12".
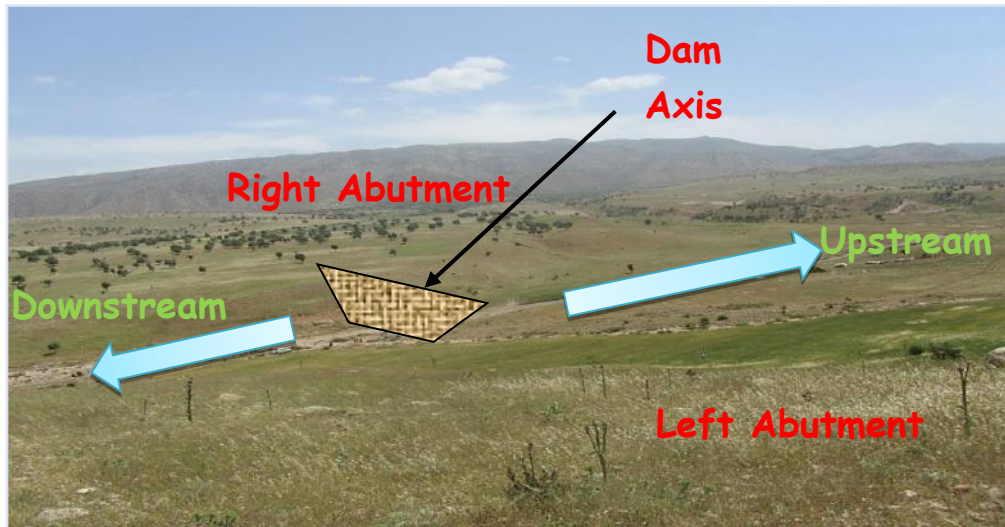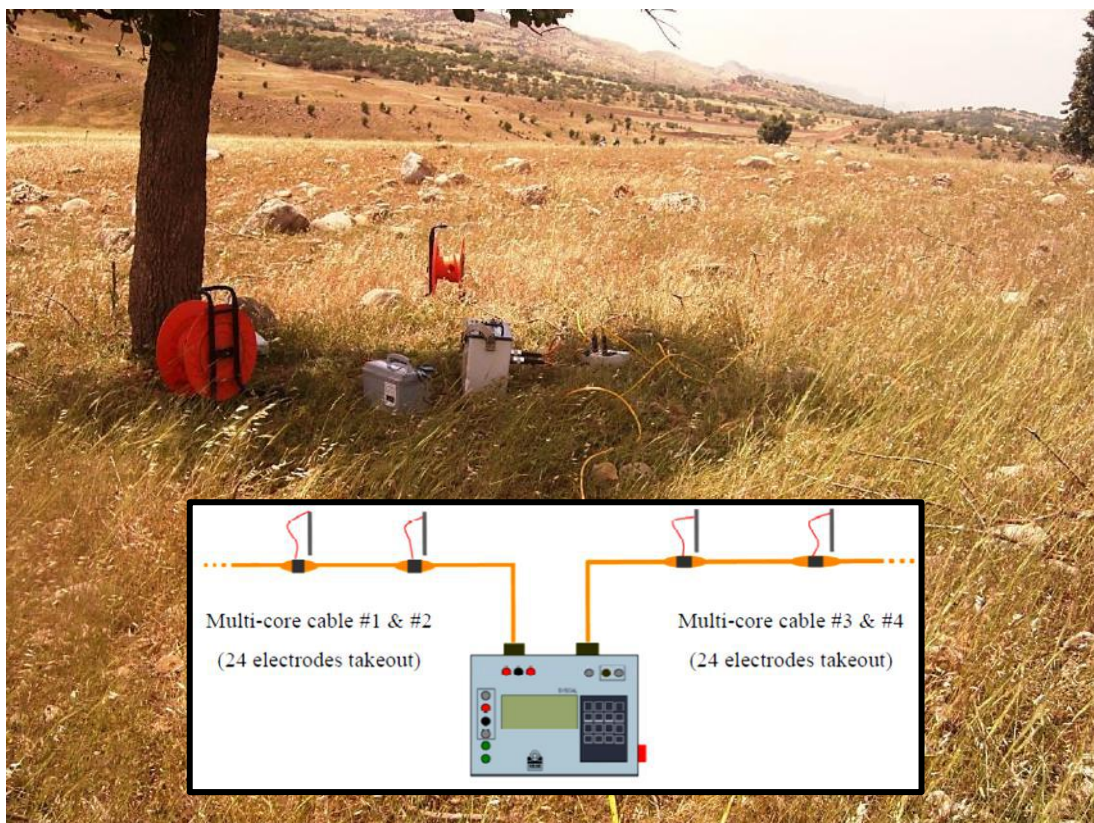
Figure 3.1: The location of the proposed dam site.

Figure 3.2: Field lay-out (https://www.iris-instruments.com/).

Figure 3.3: Image shows the field survey layout at Shaqlawa proposed dam site.

3.3 A 2-D inversion program

To convert the resistivity picture into a geological picture, some knowledge of typical resistivity values for different types of subsurface materials and the geology of the area surveyed, is important. The resulting measurements were combined with the available geological and geotechnical reports of the study area and were used to assess the structure of the near-surface geology. After the acquisition of the geophysical data, Interpretation of the resistivity results was carried out using commercial software TomoLAB® which belongs to (Geoastier Italian Company). The ERT data after collected by using a previous produces a subsurface map of the "apparent" resistivity distribution. The apparent resistivity distribution of the subsurface structure is then inverted using the commercial TomoLab® software to estimate the true resistivity structure. The inversion problem is to find resistivity values of the cells that have best fitness between the measured and calculated apparent resistivity values (Faleye and G.O. Omosuyi, 2011)

3.4 Interpretation of 2D resistivity imaging data

Profile 1 (parallel to the dam axis)

It is parallel to the proposed dam axis and running normal to the strike of the outcrops (SW - NE). The first electrode is assumed to be on the left abutment, at the coordination (X = 446262 and 446172; Y = 4026637 and 4026423 UTM). The outcrops of Injana (upper Fars) Formation occur in the area and its surrounding area. A layer of recent sediments and alluvium deposit as well as weathered product of Upper Fars formation is covering surface of the area, it has resistivity ranging from 35 to 95 Ω.m, and it is composed of boulders, gravels, sand and silt. The layer has thickness ranging from 8 to 10 m (Fig. 3.4). The second layer is representing the sandstone bed of Injana (upper Fars) Formation in the left abutment; it shows resistivity about 30 Ω.m. This layer has thickness ranging from 10 to 12 m and extends to the center of the dam axis because it has dip direction toward NE. A low resistive layer is detected at depths ranging from 8 to 10 m; it is composed of claystone, siltclay and siltstone. It has resistivity ranging from 15 to 20 Ω.m this layer is extended to the lower part of the resistivity section. This layer represents the fine materials of Injana (upper Fars) Formation.
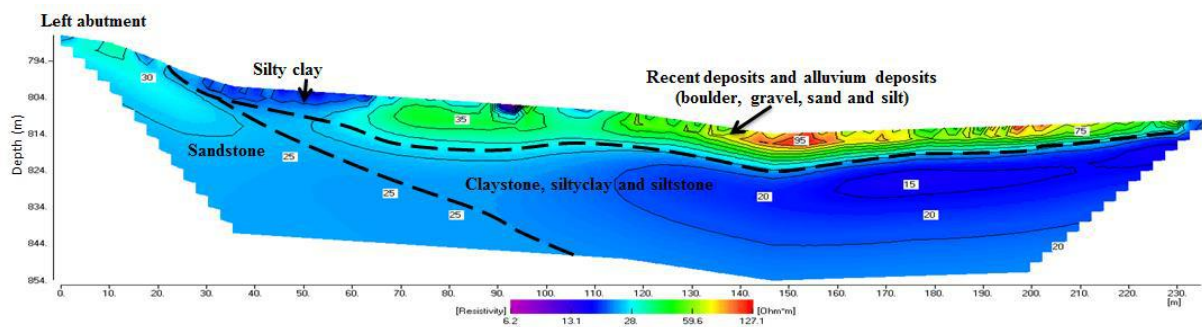

Figure 3.4: Inverse resistivity model along profile 1 which is parallel to the proposed dam axis.

Profile 2 (perpendicular to the dam axis)

It is located in the central of the valley, the first electrode is assumed to be at the upstream, at the coordination (X= 446318 and 446153; Y= 4026445 and 4026610 UTM). The profile it is normal to proposed dam axis and running parallel to the strike of the outcrops (SE-NW). The outcrops of Upper Fars Formation occur in the area and its surrounding area. In this profile three layers were recognized; the first continuous surface layer represents by top soil with resistivity ranging from 45 to 170 Ω.m (Fig 3.5). These variations in resistivity occur due to variety types of recent sediments. It is composed of boulder, gravel, sand, silt and clay with thickness ranging from 8 to 10m. The second layer represents the first constituent of upper Fars formation which is composed of claystone and siltstone with resistivity ranging from 7 to 15 Ω.m and with thickness ranging from 6 to 10m. The third layer is composed of Sandstone bed rock of Upper Fars formation with resistivity ranging from 25 to 40 Ω.m and the sandstone bed contain water.
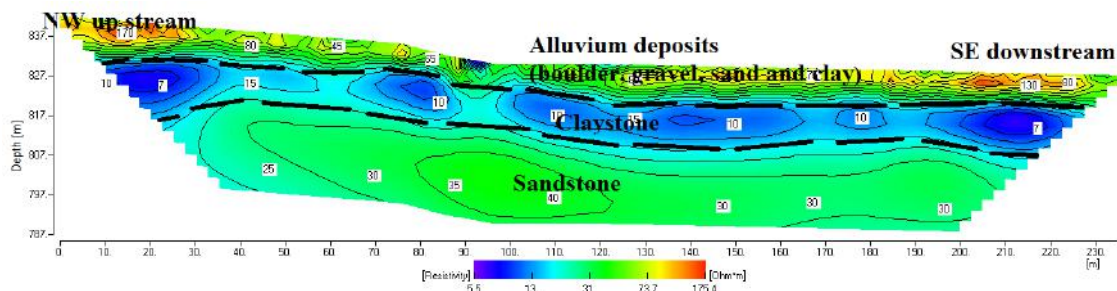

Figure 3.5: inverse resistivity model along profile 2 which is perpendicular to the proposed dam axis.

Profile 3 (Right Abutment)

It is located in the right abutment which is parallel to the strike. The first electrode is located in the left side of the profile at the coordination (X= 446335 and 446555; Y= 4026682 and 4026610 UTM). The first electrode is assumed to be on the upstream (Figures 3.1 & 3.3). In this profile three layers were recognized. The first one is representing recent sediments with resistivity ranging from 25 to 360 Ω.m in the center of the profile; it is composed of coarse sediments: boulder, gravel, pebble, sand and silt. It has thickness ranging from about 8 to 10m (Fig 3.6). And laterally in the right directions changes to top soil composed of sand which is located at the left side of profile. The second layer is composed of dry siltstone and silt clay with resistivity ranging from 20 to 40 Ω.m. The resistivity of this layer decrease towards the left to 20 Ω.m with thickness ranging from about 3 to 5m. This decreasing in the resistivity value is due to increasing fine sediments in the upper Fars constituents. The third layer is composed of compact sandstone bed rock of Upper Fars formation with resistivity ranging from 85 to 130 Ω.m and in small part the lithology changes in to fracture sandstone with resistivity about 50Ω.m.
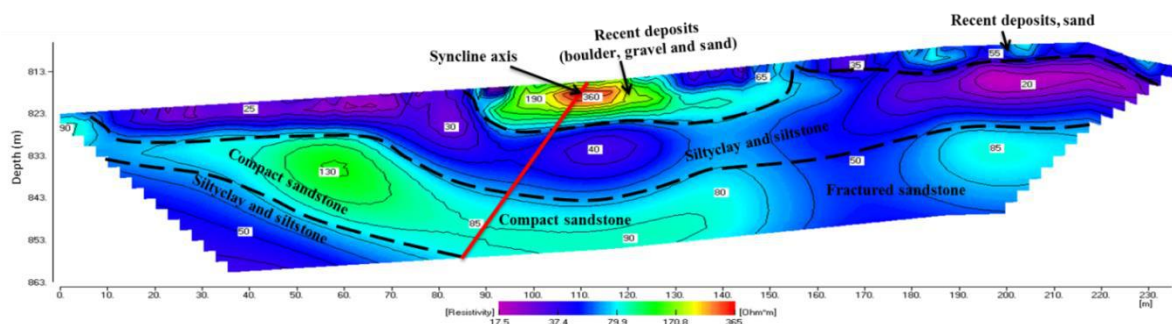

Figure 3.6: inverse resistivity model along profile 3 which is on the right abutment of proposed dam.

Chapter Four

Conclusions and Recommendations

4.1 Conclusions:

2-D Electrical Resistivity Tomography were carried out at the Shaqlawa Proposed Dam Site at Erbil Governorate, NE Iraq and the data were analyzed by using TomoLab Inversion software. The ERT investigations were conducted successfully for determine any subsurface geological deficiency that may pose a problem for the building and finally to investigate the suitability of the proposed dam site. Based on the interpretation of the 2D (ERT) data the following results obtained;

1- The top surface layer shows high to moderate resistivity ranging from 75 to more than 360 Ohm.m, it is composed mainly of coarse materials such as boulder and gravel, while in some location fine soft materials such as silty clay has been appeared. The thickness of the recent sediments is ranging from 8 to 10 m.

2- A layer of high resistivity about 30 – 130 Ohm.m, has been detected within upper Fars Formation; it is mainly composed of sandstone.

3- A layer of low resistivity has been identified which represents the fine materials deposition of the Upper Fars Formation. On left abutment of the dam. the resistivity ranging between 15 to 25 Ohm.m

4- Detecting syncline axis at profile.

5- In structural point of view there is no faults have been detected in this location as well as there is no evidence of the existence of cavities and there are no any risky sources.

4.2 Recommendations

Several bore holes have to be drill on the location of these 2D resistivity profiles especially in profile 3 at the location which is composed of fracture sandstone for comparison the direct data of the wells with those obtained from the 2D interpretation.

References

1. Bellen, R.G. R.G., H.V. Dunnington, R. Wetzel, and D.M. Morton, 1959. Lexique stratigraphique International, Vol.III, Asie. In: Dubertret, L., (director), fasc. 10c. Iraq, Cenre Nat. Reaserche Scientifique, (Paris), 333p.
2. Bernard, et. al., http://www.iris-instruments.com/training.html.
3. Bernard, J., 2003. Short Note on The Depth of Investigation of Electrical Methods. IRIS Instruments, 8p.
4. Buday, T. and S.Z. Jassim, 1984. "Final report and the regional geological survey of Iraq"; Unpubl., Report, S. O. M.Library, Vol. 2, Tectonic, Framework.
5. Buday, T. and S.Z. Jassim, 1987. The regional geology of Iraq (Tectonism, Magmatism and Metamorphism). Vol.2, Geological Survey and Mineral Investigation, Baghdad, Iraq,352p.
6. Buday, T., 1980. The regional geology of Iraq. Stratigraphy and Paleogeography. Dar Al-Kutib Publishing house, University of Mosul, Mosul, Iraq, 445p.
7. Dahlin, T. (1996) 2D Resistivity Surveying for Environmental and Engineering Applications.
8. Faleye, E.T. and G.O. Omosuyi, 2011. "Geophysical and Geotechnical characterization of foundation beds atKuchiyaku, Kuje area, Abuja, Nigeria", Journal ofemerging trends in Engineering and Applied Sciences, 2 (5), pp. 864–870.
9. Griffiths, D.H. and R.D. Barker, 1993. "Two-dimensional resistivity imaging and modeling in areas of complex geology", J. Appl. Geophysics., 29, pp. 211-226.
10. https://www.iris-instruments.com/
11. Jassim, S.Z. and J.C. Goff, 2006. Geology of Iraq (First edition). Published by Dolin, Prague and Moravian Museum, Brno, Czech Republic, 341p.
12. Keary, P., Brooks, M. and Hill, I. (2002) An Introduction to Geophysical Exploration.
13. Knodel, K., Lange, G. and Voigt, H. J., 2007. Environmental geology. Springer Berlin Heidelberg New York, 1357p.
14. Loke, M. H. (2014). Electrical Imaging Surveys for Environmental and Engineering Studies.
15. Museett, A. E. and Aftab Khan, M., 2000. Looking into the earth- An introduction to geological geophysics. Cambridge University Press, First published, 470p.
16. Reynolds, J. M. (2011). An Introduction to Applied and Environmental Geophysics.
17. Sissakian, V. K., 1997. "Geological Map of Shaqlawa area northeast Iraq", GEOSURV, Baghdad, Iraq.